Journal of Biomolecular NMR (2005) 33: 43–50
DOI 10.1007/s10858-005-1284-4


*Article*

# Fast assignment of $^{15}$N-HSQC peaks using high-resolution 3D HNcocaNH experiments with non-uniform sampling

Zhen-Yu J. Sun[a], Dominique P. Frueh[a], Philipp Selenko[a], Jeffrey C. Hoch[b] & Gerhard Wagner[a,*]

[a]*Department of Biological Chemistry and Molecular Pharmacology, Harvard Medical School, Boston, MA 02115, U.S.A.;* [b]*Department of Molecular, Microbial, and Structural Biology, University of Connecticut Health Center, Farmington, CT 06030, U.S.A.*

Received 23 May 2005; Accepted 18 July 2005

*Key words:* HNcocaNH, maximum entropy reconstruction, non-uniform sampling, sequential assignment, triple resonance experiment

**Abstract**

We describe an efficient NMR triple resonance approach for fast assignment of backbone amide resonance peaks in the $^{15}$N-HSQC spectrum. The exceptionally high resolutions achieved in the 3D HncocaNH and hNcocaNH experiments together with non-uniform sampling facilitate error-free sequential connection of backbone amides. Data required for the complete backbone amide assignment of the 56-residue protein GB1 domain were obtained in 14 h. Data analysis was vastly streamlined using a 'backbone NH walk' method to determine sequential connectivities without the need for $^{13}$C chemical shifts comparison. Amino acid residues in the sequentially connected NH chains are classified into two groups by a simple variation of the NMR pulse sequence, and the resulting 'ZeBra' stripe patterns are useful for mapping these chains to the protein sequence. In addition to resolving ambiguous assignments derived from conventional backbone experiments, this approach can be employed to rapidly assign small proteins or flexible regions in larger proteins, and to transfer assignments to mutant proteins or proteins in different ligand-binding states.

## Introduction

Protein structure determination by NMR in solution typically begins with the sequential assignment of backbone amide and carbon resonances using well-established 3-dimensional (3D) experiments (Cavanagh et al., 1996; Ferentz and Wagner, 2000). The data are analyzed manually or automatically by connecting spin systems with common (overlapping intra-residual and sequential) carbon resonances. This process can be complicated by degeneracy in $^{13}$C chemical shifts. Furthermore, for many applications such as mapping of binding sites, it may be sufficient to assign only the amide group cross peaks in the $^{15}$N Heteronuclear Single Quantum Coherence (HSQC) spectra (Bodenhausen and Ruben, 1980), without the need for $^{13}$C chemical shift information. Consequently, HNcaNH and HNcocaNH experiments (Grzesiek et al., 1993b; Weisemann et al., 1993) have been designed to achieve such amide connectivities, complementing the conventional triple resonance experiments by utilizing the superior resolution of the amide chemical shifts. Improvements of these 3D and 4D pulse sequences have been reported, including perdeuteration, homonuclear carbon decoupling or concatenation of pulse-sequence elements, that significantly enhance their sensitivity (Matsuo et al., 1996; Bracken et al., 1997; Ikegami

*To whom correspondence should be addressed. E-mail: gerhard_wagner@hms.harvard.edu

et al., 1997; Panchal et al., 2001). However, all of these experiments require days of spectrometer time, and their spectral resolution does not take full advantage of the narrow amide line-widths.

Here, we present a novel backbone amide assignment approach that is based on improved 3D HncocaNH and hNcocaNH pulse sequences and ultra high resolutions, in all indirect dimensions, obtained with non-uniform sampling (NUS) (Schmieder et al., 1993, 1994). Recently developed NUS experiments for backbone as well as side-chain resonance assignments have been shown to significantly reduce the overall measurement time by sampling only a subset of time increments while maintaining high resolution (Rovnyak et al., 2004a; Sun et al., 2005). Non-uniform sampling preserves excellent signal-to-noise ratios by sampling more densely at short evolution times when the signals are strong, and less frequently at long evolution times when signals are weaker than noise (Rovnyak et al., 2004b). As shown in the experiments described here, we have converted all evolution periods for the indirect dimensions to semi-constant time (semi-CT) evolution modules. This enables us to obtain maximum spectral resolution (as limited by line-widths) and improve sensitivity at the same time by sampling non-uniformly. Utilizing ultra-high resolution (comparable to the directly detected dimension) for all indirectly evolved dimensions, we devised a simple 'backbone NH walk' approach to establish sequential connectivities. We demonstrate this approach with the complete backbone amide assignment of the 56-residue protein GB1 domain (Gronenborn et al., 1991), with data acquired overnight (14 h) on a 750 MHz spectrometer with a conventional room-temperature probe.

## Methods

### *Pulse sequence overview*

Although our approach is applicable to both the HNcaNH and the HNcocaNH experiments, we chose to focus on the latter for its spectral simplicity and stronger sequential cross peaks, barring relaxation considerations (Panchal et al., 2001). The magnetization transfer in the HNcocaNH experiments consists of a strong sequential and a weaker intra-residual correlation pathway (Grzesiek et al., 1993b; Matsuo et al., 1996; Bracken et al., 1997; Panchal et al., 2001). The sequential pathway consists of magnetization transfers from $N_{i+1}$ to $CO_i$ via the $^1J_{NCO}$ coupling, then to $C\alpha_i$ via $^1J_{COC\alpha}$, and finally to $N_i$ via the $^1J_{NC\alpha}$ coupling. The intra-residual pathway branches off in the last step from $C\alpha_i$ back to $N_{i+1}$ via the weaker $^2J_{NC\alpha}$ coupling. Therefore, the 3D HncocaNH and hNcocaNH spectra generally contain strong sequential cross peaks and weak intra-residual diagonal peaks. The sequential cross peaks correlate amide resonances of the succeeding residue (evolved in the indirect dimensions) to the directly observed amide resonances, enabling a forward, unidirectional 'backbone NH walk'.

The pulse sequences for the NUS HncocaNH and hNcocaNH experiments, as shown in Figure 1, are identical except for the initial periods (points a–c). In the HncocaNH experiment, the first semi-CT (Grzesiek and Bax, 1993b) evolution period transfers coherences encoded with $^1H$ chemical shifts from $H_{i+1}$ to $N_{i+1}$, and is followed by an INEPT (Morris and Freeman, 1979) transfer from $N_{i+1}$ to $CO_i$. The hNcocaNH experiment includes instead a $H_{i+1}$ to $N_{i+1}$ INEPT transfer and a $^{15}N$ semi-CT evolution period that encodes $^{15}N$ chemical shifts while transferring coherences to $CO_i$. In order to maximize sensitivity, concatenations of the coherence transfer and refocusing steps are employed through out the remaining portions of the pulse sequences, except for the final WATERGATE period (Piotto et al., 1992; Sklenár et al., 1993).

In particular, a pulse scheme eliminating a 24 ms refocusing period was adopted to significantly increase the sensitivity as previously reported (Panchal et al., 2001). Specifically, the anti-phase coherence of $N_{i+1}$ with respect to $CO_i$ is not immediately refocused at point c, and becomes anti-phase with respect to $C\alpha_i$ after the $CO_i \rightarrow C\alpha_i$ coherence transfer period at point d. During the $C\alpha_i \rightarrow N_i$ coherence transfer period (points d–f), the coherence evolves to be in-phase via the $^2J_{NC\alpha}$ coupling. The length of the $C\alpha \rightarrow N$ magnetization transfer period ($2T_C$) was set to 32 ms as a demonstration for general-applications, although it can be as long as 48 ms for maximum sensitivity gain for small proteins such as GB1. Since $C\alpha$ magnetization is transverse during this period, a $C\alpha$ selective pulse was

additionally employed (at point e) to allow for Cβ decoupling that further improves sensitivity (Matsuo et al., 1996).

*Semi-constant $^{15}N$ evolution periods*

Compared with previous reported HNcaNH and HNcocaNH pulse sequences, the major modification is inclusion of the $^{15}N$ semi-CT evolution periods. The length of a typical $^{15}N$ constant evolution period ($t_{max}$) is 24.8 ms, which yields a maximum intrinsic spectral resolution of 40 Hz. The use of $^{15}N$ semi-CT periods is necessary for achieving higher spectral resolution when employing NUS schedules to match the narrow $^{15}N$ line-widths. For protein GB1, a $^{15}N$ intrinsic resolution of 26 Hz was obtained corresponding to 0.34 ppm on a 750 MHz spectrometer. For even narrower peaks (e.g. in unfolded protein), this can potentially be improved further by using a NUS schedule with extended maximum evolution times.

The first $^{15}N$ semi-CT evolution period in Figure 1b is designed to perform four tasks simultaneously: chemical shift evolution for $N_{i+1}$, refocusing of $H_{i+1}$ anti-phase coherence, coherence transfer from $N_{i+1}$ to $CO_i$, and Cα decoupling. The four initial delays were set to yield a transfer time of 24.8 ms (relaxation optimized). The four time increments were calculated so that the transfer time was gradually increased to a final value of 33.2 ms ($1/2J_{NCO}$) for maximal transfer efficiency with increasing $^{15}N$ evolution time.

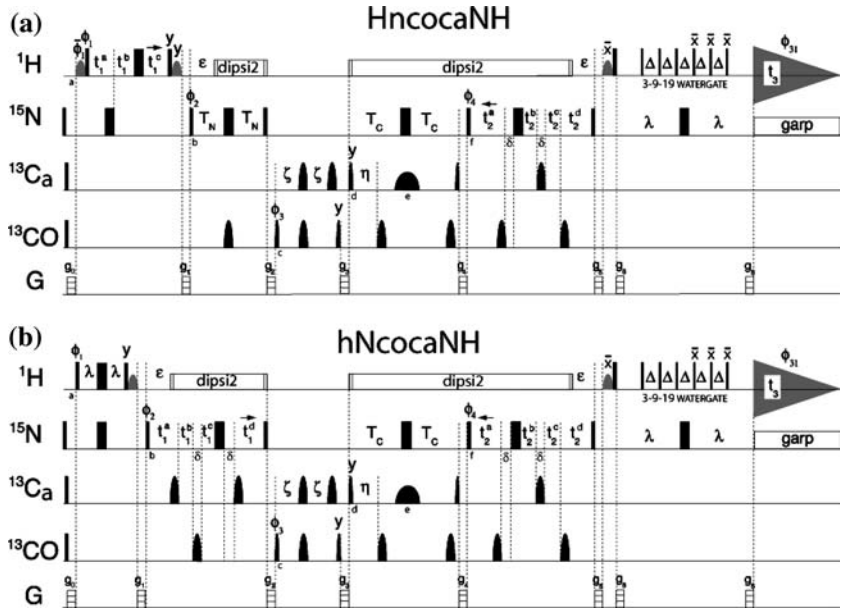


*Figure 1.* Pulse schemes for the 3D NUS (a) HncocaNH and (b) hNcocaNH experiments (identical after points c). Narrow and wide bars indicate 90° and 180° hard pulses, narrow and wide hemi-ellipses indicate 90° (GaussCascadeQ5) and 180° (GaussCascadeQ3) shaped pulses respectively (Emsley and Bodenhausen, 1992). Shaded hemi-ellipses indicate water flip-back pulses (Grzesiek and Bax, 1993a). The shaped 180° pulse at points e has a bandwidth of either 22 ppm or 31 ppm for Cα and Cα+ selective pulse, respectively. The delays are: $\varepsilon = 5.5$ ms; $\zeta = \eta = 4.5$ ms; $\lambda = 2.3$ ms; $\Delta = 140$ μs; $T_N = 12.4$ ms. $T_C$ is set to 16 ms. The short delay $\delta = 210$ μs compensates for the $^{13}C$ 180° pulse. The delays and increments for $^1H$ $t_1$ semi-CT period in HncocaNH are: $t_1^a = t_1^c = 2.3$ ms; $t_1^b = 0$ ms; $\Delta t_1^a = 1/2\ SW_H + 0.45\ ms/n_{1max}$; $\Delta t_1^b = 1/2\ SW_H - 2.75\ ms/n_{1max}$; $\Delta t_1^c = -2.3\ ms/n_{1max}$. The parameters for the $^{15}N$ $t_1$ semi-CT period in hNcocaNH are: $t_1^a = t_1^d = 12.4$ ms; $t_1^b = t_1^c = 0$ ms; $\Delta t_1^a = 1/2\ SW_N - 12.4\ ms/n_{1max}$; $\Delta t_1^b = 16.6\ ms/n_{1max}$; $\Delta t_1^c = 1/2\ SW_N - 16.6\ ms/n_{1max}$; $\Delta t_1^d = -12.4\ ms/n_{1max}$. The parameters for the $^{15}N$ $t_2$ semi-CT periods are: $t_2^a = t_2^d = 13.7$ ms; $t_2^b = t_2^c = 0$ ms; $\Delta t_2^a = -13.7\ ms/n_{2max}$; $\Delta t_2^b = 1/2\ SW_N - 15.7\ ms/n_{2max}$; $\Delta t_2^c = 15.7\ ms/n_{2max}$; $\Delta t_2^d = 1/2\ SW_N - 13.7\ ms/n_{2max}$. The values $n_{1max}$ and $n_{2max}$ are the maximum incremented points for the respective dimensions. All pulses are applied along $x$, unless specified otherwise. Phase cycling in both experiments are as follows: $\phi_1 = x$; $\phi_2 = x, -x$; $\phi_3 = 2(x), 2(-x)$; $\phi_4 = 4(x), 4(-x)$; $\phi_{31}$(receiver) $= x, -x, -x, x, -x, x, x, -x$. For hNcocaNH, quadrature detections in $t_1$ and $t_2$ are achieved by incrementing $\phi_2$ and $\phi_4$ according to States-TPPI respectively (Marion et al., 1989). For HncocaNH, quadrature detection in $t_1$ ($^1H$) uses States method for $\phi_1$ that shifts the $^1H$ signals by half the spectral width, and in $t_2$ ($^{15}N$) regular States-TPPI for $\phi_4$. The $^1H$ carrier is centered on water resonance, and the $^{15}N$ carrier is placed at 118 ppm. The $^{13}C$ carrier is placed on CO resonance at 176 ppm until point d where it is switched to Cα. The $^1H$ DIPSI2 decoupling (Shaka et al., 1988) uses a 15 kHz decoupling RF field, and the $^{15}N$ GARP decoupling (Shaka et al., 1985) uses a 5.9 kHz RF field.

The second $^{15}N$ semi-CT periods in both Figures 1a and b are designed similarly to achieve $N_i$ evolution, C$\alpha$ refocusing, $N_i \rightarrow H_i$ coherence transfer, and CO decoupling simultaneously. But the initial and final magnetization transfer time were set to 27.4 ms (relaxation optimized) and 31.4 ms (transfer efficiency optimized), respectively.

*Data acquisition and processing*

The pulse sequences were developed in part using a $^{15}N/^{13}C$-labeled GFL (Gly–Phe–Leu) peptide standard (Cambridge Isotope Laboratories, Andover, MA), and tested using a 2 mM sample of uniformly $^{15}N/^{13}C$-labeled protein GB1 domain (6.4 kDa) in 20 mM $KPO_4$ buffer with 150 mM NaCl, pH 6.4. All data were acquired at 25 °C using a conventional room-temperature probe on a Bruker Avance spectrometer with a $^1H$ operating frequency of 750 MHz, with a recycling delay of 1 s. The NUS HncocaNH data were acquired using a 1400-complex point sampling schedule with 4 scans per FID in 8 h. The maximum increments in the NUS schedule are 180 and 100 for the indirect $^1H$ and $^{15}N$ dimensions, all centered in the amide region with the spectral widths being 4498 Hz and 2583 Hz respectively. The NUS hNcocaNH data of protein GB1 were acquired using a 1024-complex point sampling schedule with 4 scans per FID in 5.6 h. The maximum increments in the NUS schedule are 100 for both indirect $^{15}N$ dimensions, with spectral widths of 2583 Hz. The directly observed $^1H$ dimension for both experiments has a spectral width of 8993 Hz (centered at 4.7 ppm) with 512 complex points. To achieve a similar resolution with conventional uniform sampling, the total measuring time would have needed to be extended from the current 14 h to 158 h (6.6 days).

Data processing was carried out using the maximum entropy reconstruction algorithm of the Rowland NMR Toolkit (Hoch and Stern, 1996), on a Dell computer with dual Xenon 3.0 GHz processors running under Fedora Core 1 Linux operating system. The processing time (using the parameters DEF = 5 and LAMBDA = 0.1) was 21 min for the NUS HncocaNH data set with a final matrix size of 512 × 256 × 450 points, and 11 min for NUS hNcocaNH data with a final matrix size of 256×256×450 points. The resulting NMR spectra were analyzed using the software CARA (available from http://www.nmr.ch/) (Keller, 2004). CARA provides a very useful interface for implementing the 'backbone NH walk' algorithm using the 3D HNcocaNH data. However, the same method may be adopted using other software such as nmrView and Sparky, and can be readily automated with scripts or stand-alone programs.

## Results

*Sequential connectivity in GB1*

The process of establishing sequential connectivity of the 56-residue protein GB1 domain using 'backbone NH walk' is illustrated in Figure 2. Three spectra of the 2D $^{15}N$-HSQC, 3D NUS HncocaNH and hNcocaNH experiments are simultaneously displayed using CARA. Marking a spin-system (peak identifiers) in the HSQC spectrum will bring up the corresponding plane strips in the HncocaNH and hNcocaNH spectra, centered with the diagonal peak. The $^{15}N$ and $^1H$ chemical shift values of the sequential cross peaks in the HncocaNH and hNcocaNH strips are highly accurate given the ultra-high resolutions, and are then used to locate the spin-system of the succeeding residue in the HSQC spectrum. As shown by the arrows in Figure 2, each sequential connection involves two separate steps using HncocaNH and hNcocaNH data respectively, resembling a bipedal walking process. The dotted lines in the HSQC spectrum in Figure 2 show a chain of 9 spin-systems that have been sequentially connected using this simple 'backbone NH walk' method, without any need for strip comparison.

As in a conventional sequential assignment procedure, 'backbone NH walks' terminate at a proline or the C-terminal residue, or when two (or more) NH peaks are unresolved in the HSQC spectrum. For protein GB1, three spin-system chains were identified, with lengths of 26 (chain A), 28 (chain B) and 5 (chain C) residues, respectively. Chain A is clearly terminated with the C-terminal residue (there is no proline residue present). Chain B is looped back to an unresolved peak-pair (residues Lys4 and Lys31), and is linked with the C-terminus of chain C. Based on these characteristics, all backbone NH resonances of protein GB1 were unambiguously assigned using

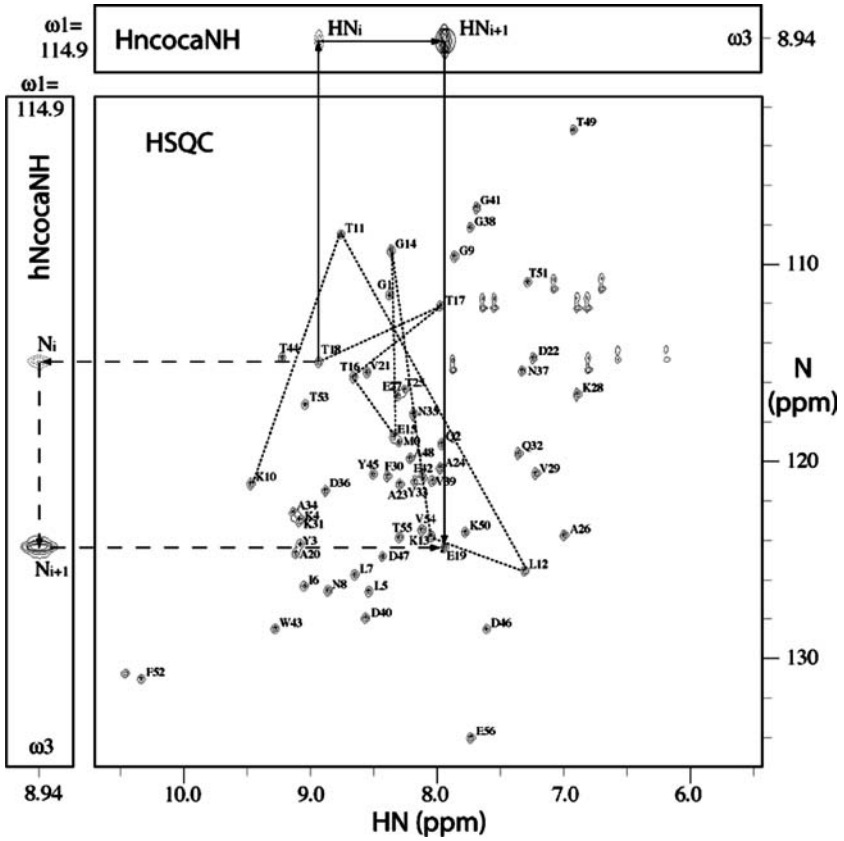


*Figure 2.* A diagram illustrating the 'backbone NH walk' method for assigning the polypeptide amide resonances. The tracing of sequentially connected residues (Lys10 to Thr18) in a segment of protein GB1 domain is shown with dotted lines in the $^{15}$N-HSQC spectrum. The $^{1}$H and $^{15}$N chemical shift values of the succeeding residues are obtained from the sequential cross peaks in the HncocaNH and hNcocaNH spectra. The solid-line and dashed-line arrows relating to the top and left strip panels demonstrate $^{1}$H and $^{15}$N connectivities, respectively, leading from residue Thr18 to Glu19.

the 3D NUS HncocaNH and hNcocaNH data only. For larger proteins, with increased number of sequentially connected chains as a result of more unresolved NH peaks and/or proline residues, it is desirable to obtain the amino acid type information from the CcoNH experiment (Logan et al., 1992; Grzesiek et al., 1993a), or use a simple method described below.

*Sequential assignment using 'ZeBra' patterns*

As shown in Figure 1, the Cα selective 180° pulse (with 22 ppm bandwidth centered at 55 ppm) in the middle of the Cα → N transfer period removes the Cα/Cβ J-coupling. However, the Cβ spins of serine residues are also inverted by the Cα selective pulse (Figure 3a) and remains coupled to Cα. Likewise, by varying the offset (51 ppm) and bandwidth (31 ppm) of this $^{13}$C shape pulse, we can selectively refocus Cα and invert the Cβ resonances in the shaded region shown in Figure 3a, resulting in the loss of Cβ decoupling for certain types of amino acids. Serendipitously, when the duration of the Cα → N magnetization transfer period ($2T_C$) is approximating $1/J_{C_\alpha C_\beta}$ (27 ms), the effect of the Cα/Cβ coupling results only in a sign inversion for the Cα coherences. We can thus classify amino acid residue types into two groups according to their responses to this (Cα+) selective pulse affecting the Cα plus a subgroup of the Cβ resonances. The one-letter abbreviation codes for amino acids Asp/Asn ('B') and Glu/Gln ('Z') are chosen to represent the two groups of amino acids that have clearly separated average Cβ chemical shifts. The group 'B' includes Asp, Asn, Leu, Phe, Tyr, and Ile residues, and the group 'Z' includes Glu, Gln, Thr, Met, Lys, Val, Pro, Arg, His, Trp, Ala (plus Gly and Ser) residues. The Cys

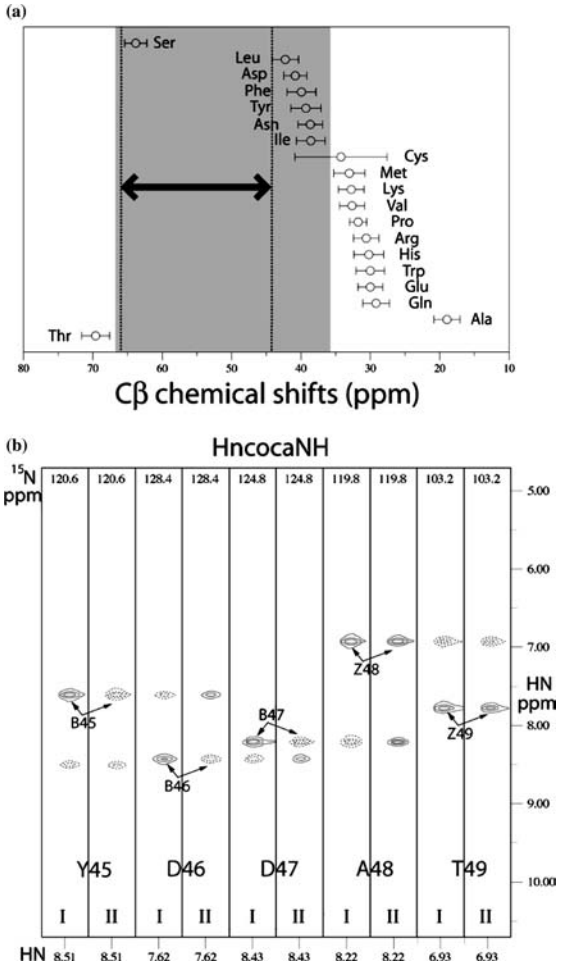


*Figure 3.* (a) Statistical values of the Cβ chemical shift distribution with standard deviations represented by error bars (obtained from BioMagResBank). The region between the dotted lines indicates the spectral range affected by the Cα selective pulse, while the region shaded in grey is affected by the Cα+ selective pulse as described in the main text. Residues inside the shaded region (except Ser) form the 'B' group, while those outside (except Cys) plus Gly and Ser belong to the 'Z' group, as explained in the main text. (b) Example of strips from HncocaNH spectra acquired using a Cα (experiment I) or a Cα+ (experiment II) selective pulse during the Cα → N magnetization transfer period. Positive peaks are represented by solid contours, and negative peaks by dotted contours. For residues of the 'B' group, the more intense cross peaks correlating the succeeding residue (indicated by the arrows) have opposite signs between the two experiments. The resulting 'ZeBra' stripe pattern 'BBBZZ' is consistent with this short stretch of amino acid sequence 'YDDAT'.

residues straddle both groups unless their redox states are predetermined. This classification of amino acids as 'Z'/'B' types can be used to construct 'Z/B' residue annotation ('ZeBra') patterns for any given protein sequence.

As indicated by arrows in Figure 3b, the sequential cross peaks of residues of group 'B' have opposite signs in the two HncocaNH spectra acquired using different Cα selective pulses. In this way, the 'ZeBra' patterns can be determined for all spin-system chains connected by the 'backbone NH walks', and utilized for unambiguous assignments. In the case of protein GB1, using the HncocaNH data re-acquired with a Cα+ selective pulse, chain A and chain B can be readily assigned according to their 'ZeBra' patterns that are unique in the protein sequence. The assignment of the shorter chain C is also consistent with six possible matches using its 'ZeBra' pattern. This approach of using 'ZeBra' pattern obtained from all residues is more informative compared to a triplet identification method (Panchal et al., 2001) which depends only on the glycine and proline residues.

## Discussion

The high-resolution 3D NUS HncocaNH and hNcocaNH data required for 'backbone NH walk' sequential assignment can be acquired in a short experimental time (overnight). However, the use of the 3D instead of the 4D HNcocaNH data gives rise to uncertainties in identifying spin-systems of the succeeding residues when encountering unresolved NH peaks. A 3D HNcocaNH experiment using the reduced-dimensionality (RD) method (Szyperski et al., 1993; Simorre et al., 1994; Freeman and Kupce, 2003) to simultaneously evolve the $N_{i+1}$ and $H_{i+1}$ spins has been reported to remove such ambiguity (Bracken et al., 1997). We have obtained a RD-HNcocaNH data set (acquired in 8 h) for protein GB1 but deemed it unnecessary for the 'backbone NH walk' method. This is because the very $H_{i+1}N_{i+1}$ correlations can be elucidated by analyzing the $H_iN_i$ diagonal peaks for the same set of amino acid residues.

To assess spectral crowding in the $^{15}$N-HSQC spectra of larger proteins, a survey was conducted using chemical shift data deposited in the BioMag ResBank (http://www.bmrb.wisc.edu). Assuming upper limit line-widths of 18 and 20 Hz for $^{1}$H and $^{15}$N on a 750 MHz spectrometer, 90% of non-complexed protein molecules with 51–100 residues (476 surveyed) would have 3.8 unresolved NH

peaks on average, or 5.0% of the total backbone amide peaks. These numbers increase to 8.4 peaks, or 7.3% for proteins with 101–150 residues (518 surveyed), and 15 peaks, or 9.4% for proteins with 151–200 residues (193 surveyed). The remaining 10% of the proteins may include unfolded proteins or large unstructured regions with sharper peaks and require separate analyses. It should be noted, however, that unresolved NH peaks contain information of possible chain connections that can be sorted out when combined with 'ZeBra' pattern matching for sequential assignments. On average, spin-system chains containing seven or more residues can be uniquely mapped to the protein sequence according to their 'ZeBra' patterns. Overall, this inspection of the chemical shift data base is encouraging and indicates that the 'backbone NH walk' and 'ZeBra' pattern matching methods should work well for proteins of less than 15 kDa, as well as most proteins around 20 kDa.

We envisage many useful applications for this robust and simple NH resonance assignment approach. In addition to resolving ambiguities in conventional triple-resonance experiment data, the sequentially connected spin-system chains can be used as error-free initial inputs for existing manual and automated sequential assignment strategies. In combination with the NUS RD-HCcoNH experiments (Sun et al., 2005), it is also possible to obtain backbone and side-chain (aliphatic) resonance assignment for small proteins using a minimal number of short experiments. Moreover, backbone amide assignment alone is very important for studying protein complexes and ligand binding. It is relatively straightforward to transfer known backbone NH assignments to proteins in a complex (especially useful for tight complexes in slow-exchange on the NMR time scale) or mutant proteins using the 3D NUS HNcocaNH experiments. This method could also dramatically shorten the experimental time for assigning unfolded proteins (Bhavesh et al., 2001) or flexible region of large proteins (Juneja et al., 2002) in proteomic studies. Currently we are extending this assignment approach to larger proteins (MW > 20 kDa) using deuteration (Grzesiek et al., 1993b; Matsuo et al., 1996) and additional sensitivity enhancing techniques, such as TROSY(Pervushin et al., 1997).

## Acknowledgements

This research was supported by the National Institute of Health (grants GM47467 and RR00995). We are grateful to Dr M. Roehrl for the GFL peptide test sample.

## References

Bhavesh, N.S., Panchal, S.C. and Hosur, R.V. (2001) *Biochemistry*, **40**, 14727–14735.

Bodenhausen, G. and Ruben, D.J. (1980) *Chem. Phys. Lett.*, **69**, 85–189.

Bracken, C., Palmer, A.G. III and Cavanagh, J. (1997) *J. Biomol. NMR*, **9**, 94–100.

Cavanagh, J., Fairbrother, W.J., Palmer, A.G. III and Skelton, N.J. (1996) *Protein NMR Spectroscopy: Principles and Practice*, Academic Press, New York, NY.

Emsley, L. and Bodenhausen, G. (1992) *J. Magn. Reson.*, **97**, 135–148.

Ferentz, A.E. and Wagner, G. (2000) *Q. Rev. Biophys.*, **33**, 29–65.

Freeman, R. and Kupce, E. (2003) *J. Biomol. NMR*, **27**, 101–113.

Gronenborn, A.M., Filpula, D.R., Essig, N.Z., Achari, A., Whitlow, M., Wingfield, P.T. and Clore, G.M. (1991) *Science*, **253**, 657–661.

Grzesiek, S., Anglister, J. and Bax, A. (1993a) *J. Magn. Reson.*, **B101**, 114–119.

Grzesiek, S., Anglister, J., Ren, H. and Bax, A. (1993b) *J. Am. Chem. Soc.*, **115**, 4369–4370.

Grzesiek, S. and Bax, A. (1993a) *J. Am. Chem. Soc.*, **115**, 12593–12594.

Grzesiek, S. and Bax, A. (1993b) *J. Biomol. NMR*, **3**, 185–204.

Hoch, J.C. and Stern, A.S. (1996) *NMR Data Processing*, Wiley-Liss, New York, NY.

Ikegami, T., Sato, S., Wälchli, M., Kyogoku, Y. and Shirakawa, M. (1997) *J. Magn. Reson.*, **124**, 214–217.

Juneja, J., Bhavesh, N.S., Udgaonkar, J.B. and Hosur, R.V. (2002) *Biochemistry*, **41**, 9885–9899.

Keller, R.L.J. (2004) *The Computer Aided Resonance Assignment Tutorial*, Cantina Verlag, Goldau, CH.

Logan, T.M., Olejniczak, E.T., Xu, R.X. and Fesik, S.W. (1992) *FEBS Lett.*, **314**, 413–418.

Marion, D., Ikura, M., Tschudin, R. and Bax, A. (1989) *J. Magn. Reson.*, **85**, 393–399.

Matsuo, H., Kupce, E., Li, H. and Wagner, G. (1996) *J. Magn. Reson. B*, **111**, 194–198.

Morris, G.A. and Freeman, R. (1979) *J. Am. Chem. Soc.*, **101**, 760–762.

Panchal, S.C., Bhavesh, N.S. and Hosur, R.V. (2001) *J. Biomol. NMR*, **20**, 135–147.

Pervushin, K., Riek, R., Wider, G. and Wüthrich, K. (1997) *Proc. Natl. Acad. Sci. USA*, **94**, 12366–12371.

Piotto, M., Saudek, V. and Sklenár, V. (1992) *J. Biomol. NMR*, **2**, 661–665.

Rovnyak, D., Frueh, D.P., Sastry, M., Sun, Z.Y., Stern, A.S., Hoch, J.C. and Wagner, G. (2004a) *J. Magn. Reson.*, **170**, 15–21.

Rovnyak, D., Hoch, J.C., Stern, A.S. and Wagner, G. (2004b) *J. Biomol. NMR*, **30**, 1–10.
Schmieder, P., Stern, A.S., Wagner, G. and Hoch, J.C. (1993) *J. Biomol. NMR*, **3**, 569–576.
Schmieder, P., Stern, A.S., Wagner, G. and Hoch, J.C. (1994) *J. Biomol. NMR*, **4**, 483–490.
Shaka, A.J., Barker, P.B. and Freeman, R. (1985) *J. Magn. Reson.*, **64**, 547–552.
Shaka, A.J., Lee, C.J. and Pines, A. (1988) *J. Magn. Reson.*, **77**, 274–293.
Simorre, J.P., Brutscher, B., Caffrey, M.S. and Marion, D. (1994) *J. Biomol. NMR*, **4**, 325–333.
Sklenár, V., Piotto, M., Leppik, R. and Saudek, V. (1993) *J. Magn. Reson.*, **A102**, 241–245.
Sun, Z.Y., Rovnyak, D., Park, S., Stern, A.S., Hoch, J.C. and Wagner, G. (2005) *J. Biomol. NMR*, **32**, 55–60.
Szyperski, T., Wider, G., Bushweller, J.H. and Wüthrich, K. (1993) *J. Am. Chem. Soc.*, **115**, 9307–9308.
Weisemann, R., Rüterjans, H. and Bermel, W. (1993) *J. Biomol. NMR*, **3**, 113–120.